TOPOLOGY OPTIMIZATION METHOD APPLIED TO OBTAIN IMAGES FROM ELECTRICAL IMPEDANCE TOMOGRAPHY TECHNIQUE

Cícero Ribeiro de Lima
Department of Mechatronic and Mechanical Systems Engineering – University of São Paulo
Av. Prof. Mello Moraes, 2231, São Paulo – SP, 05508-900, Brazil
cicerorl@usp.br

Emílio Carlos Nelli Silva
Department of Mechatronic and Mechanical Systems Engineering – University of São Paulo
Av. Prof. Mello Moraes, 2231, São Paulo – SP, 05508-900, Brazil
ecnsilva@usp.br

Raul Gonzalez Lima
Department of Mechanical Engineering – University of São Paulo
Av. Prof. Mello Moraes, 2231, São Paulo – SP, 05508-900, Brazil
rauglima@usp.br

Abstract. *The Electrical Impedance Tomography (EIT) is a recent monitoring technique of biological tissues that allows us to obtain images of a transversal plane in any section of human body. The images are generated from voltage values measured around the plane section of human body. These voltages are obtained by applying an alternated sequence of low amplitude electrical currents in according to an excitation pattern (adjacent or diametral). The EIT deals with inverse problem solution. The main objective of the current work is to study the application of Topology Optimization Method (TOM) to obtain images of body section by using EIT. The problem of applying TOM to obtain images consists in finding a conductivity distribution in the body section domain that minimizes the difference between electric potential measured on electrodes and electric potential calculated by using a computational model. TOM allows us to include several constraints, which reduces the solution space expected in tomography examination. The solution of the topology optimization problem is obtained by combining Finite Element Method (FEM) and Sequential Linear Programming (SLP). To illustrate the implementation of the method, image reconstruction results obtained by using voltage numerical data of well-know domains are shown.*

Keywords*. electrical impedance tomography, topology optimization, mechanical ventilation, finite element.*

1. Introduction

During the last half of century XX, modern techniques have been developed to observe the interior of human body without the necessity of a lot invasive surgical interventions. Ever since, the tomography techniques became the most important way (commercially) to obtain medical images. The tomography techniques can obtain the image of the section of human body by obtaining information of a series of measurements in several directions on the plane section. Among all of them, the tomographies by x-ray and by magnetic resonance are the most common techniques. However, in the last 10 years approximately, another technique called Electric Impedance Tomography (EIT) has been studied as an interesting alternative for obtaining images in clinical applications. Essentially, EIT consists in obtaining images that represent any transversal plane section of human body (head, thorax, thigh, etc), where each pixel in the image is related to its corresponding value of electrical conductivity or resistivity. On the section of body to be studied, a sequence of low frequency alternate electrical currents is applied through electrodes positioned around of the patient's body and aligned in a plane corresponding to a transverse section of the body (Cheney, et. al., 1999), as illustrated in Fig. 1.

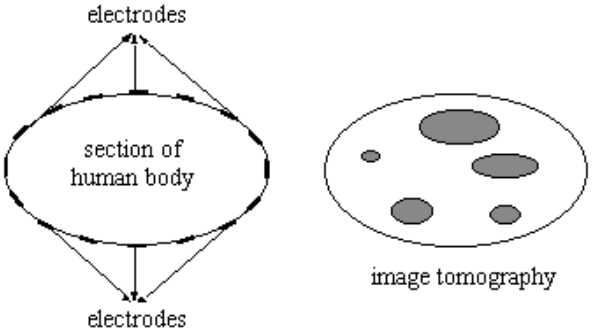

Figure 1 – Electrodes positioned around of the body.

In EIT the solution of the inverse problem is executed (Cheney and Isaacson, 1991), that is, if given the applied

current and measured voltages in the electrodes, it tries to find the conductivity (or resistivity) distribution in the section of human body. Then, by injecting known amounts of current, according to a excitement pattern (adjacent or diametral) (Isaacson et al., 1992), and measuring the resulting electrical potential field (voltages) at electrodes on the boundary of the body, it is possible to estimate and construct a map of the conductivity distribution of the region of the body probed by the currents.

The EIT resolution is largely controlled by the number of electrodes attached simultaneously to a patient and although it is expected to have relatively poor resolution compared to another tomography technique the EIT has some very attractive features for clinical applications such as monitoring lung fluid, monitoring of heart function and blood flow, detecting tumors, and other (Holder, 1993). The technology for doing electrical impedance imaging is safe and cheaper than other techniques as computer tomography and resonance magnetic tomography (Barber, 1990). Moreover an EIT device is short and portable which allows its installation for continuous monitoring of bedridden patients. This features is extremely important to avoid dangerous patient transportation from ICU (Intensive Care Unit) to the exam room. In this technique the patient does not have exposition to any type of radiation, just to the low current levels that do not cause any harm to the patient, and therefore could be applied to the human body for a long time (Amato, 2001).

This work presents a study and preliminary results of the application of Topology Optimization Method (Bendsøe and Kikuchi, 1988) to obtain images of section of the body by using EIT technique. The Topology Optimization Method (TOM) tries to find systematically a material distribution inside of a design domain (the section of body), to minimize (or maximize) an objective function requirement satisfying specified constraints. In the case of the image reconstruction problem, the main advantage of TOM is to allow us to include several constraints, which reduces the solution space expected in tomography examination. The problem of applying TOM to obtain an image of body section consists in finding a conductivity distribution in the body section domain that minimizes the difference between electric potential measured on electrodes and electric potential calculated by using a computational model. Conductivity distribution is directly related to material distribution inside of the domain and thus to the voltage values measured on electrodes positioned at domain boundary. The solution of the topology optimization problem is obtained by combining Finite Element Method (FEM) and an optimization algorithm called Sequential Linear Programming (SLP).

The next sections of the paper are organized as follow. In the section 2 some reconstruction methods for EIT are mentioned. Section 3 describes in more details the Topology Optimization Method and in section 4 the topology optimization problem formulated to obtain image by using EIT is defined. Image reconstruction results by using voltage numerical data of well-know domains are shown in section 5. Finally, section 6 draws the conclusions.

2. Electrical Impedance Tomography

The first studies and theoretical formulations for implementation of image reconstruction algorithms that constructed the foundation for EIT in practical applications medicine emerged in the 80's years at the University of Sheffield (England). Researchers of this university studied the EIT technique and described the reasons of the interest for its practical application in medicine such as, for instance, the monitoring of lung, heart and gastric functions (Holder, 1993). They are practically the pioneers in the formulation of theories and data that based EIT until the present moment. The development and the patent of the first commercial EIT device belonged to them. This device is based on the Backprojection method (Santosa and Vogelius, 1990) and it has a scheme called APT system (Applied Potencial Tomography), which is composed by a simple source of electric current with 16 electrodes and it uses the adjacent pattern for application of the electrical current (Barber and Brown, 1984). In APT system, current is passed through two adjacent electrodes and then voltage on all the other electrodes is measured. Next, current is generated between another pair of adjacent electrodes, and so on, until all adjacent pairs have served as "driver pairs". This approach has the advantage of simplicity of design, but its resolution is intrinsically limited. Although this APT system just allows us to obtain images of low resolution, it has been used in studies of several medical procedures as the monitoring of the blood flow in the thorax and lung problems (Holder, 1993), for instance. In the 90's years, other researchers present other designs and experimental instrumentations that evaluate the Backprojection method to use in EIT (Guardo et al., 1991). They also described the importance of the experimental results obtained by using so-called phantoms (Paulson et al., 1992). In the present time, researchers of Rensselear Polytechnic Institute (USA) designed and built another EIT device that it has a scheme called ACT system (Adaptive Current Tomography) with 32 electrodes, which is able to obtain 20 static images per second (Cheney et al., 1990; Cheney et al., 1999). This device uses a "fast" method for image reconstruction, which is based on the One-Step Newton method (Simske, 1987). In Brazil, the development of a EIT device has been studied by researchers of the University of São Paulo in a thematic project whose objective is to study the algorithms reconstruction for EIT to monitor accurately the mechanical ventilation of lungs (Amato, 2001).

3. Topology Optimization Method

Topology Optimization Method (Bendsøe and Kikuchi, 1988) is a generic and systematic and iterative method that combines optimization algorithms with an analysis method, in general the FEM, to distribute a material inside of a fixed design domain (region limited by the boundary conditions and that it will contain the desired image) to minimize or to maximize a specified objective function. In the Topology Optimization Method (TOM), the fixed design domain is divided on several finite elements and its FEM mesh of the domain is not changed during the optimization process. The material in each point of the fixed design domain can vary of a material type A to another one type B, assuming

intermediate materials between A and B in according to a law called material model, that defines the mixture in micro-scale of two or more materials.

In this work, the material model used is known as Density Method (Bendsøe and Sigmund, 1999). Therefore, considering the domain has been discretized in N finite elements, the conductivity properties ($\mathbf{c}_i$) of each element can be given in the following way:

$$\mathbf{c}_i = \rho_i^{\,p}\mathbf{c}_A + (1-\rho_i)^p\,\mathbf{c}_B, \quad \text{com}: \quad 0 \le \rho_i \le 1,\ i = 1...N \tag{1}$$

where $\mathbf{c}_A$ and $\mathbf{c}_B$ are the conductivity properties of the basic materials that compose the domain. In that case, the material A could be air, for instance, and the material B could be the tissue of the lungs. The values of each ρ_i can vary of 0 (indicating the presence of the material B) to 1 (indicating the presence of the material A). Intermediate values between 0 and 1 indicate the mixture of the two materials (gray scale) and they are not interesting in the final result. However, these values should be avoided by use of penalization parameter *p*, whose value must be adjusted (Bendsøe and Sigmund, 1999).

The process of topology optimization is started with a distribution uniform of design variables for whole domain and it is altered along the iterations until convergence of the process, which it occurs when the objective function is satisfied. The solution of optimization problem in the TOM is obtained numerically by iterative algorithm optimization whose steps are shown in Fig. 2. The FEM model of the design domain is supplied to the algorithm as initial data. By the analysis of the FEM model, the voltages are calculated, allowing us to obtain the objective function and constraints values. In next step, the optimization is realized, but it requires sensitivity analysis before, that is, the calculus of gradients of the objective function and constraints relative to design variables. The optimization algorithm supplies a new material distribution, which is updated in the FEM analysis. The iteration steps continue until the convergence is achieved for the objective function value.

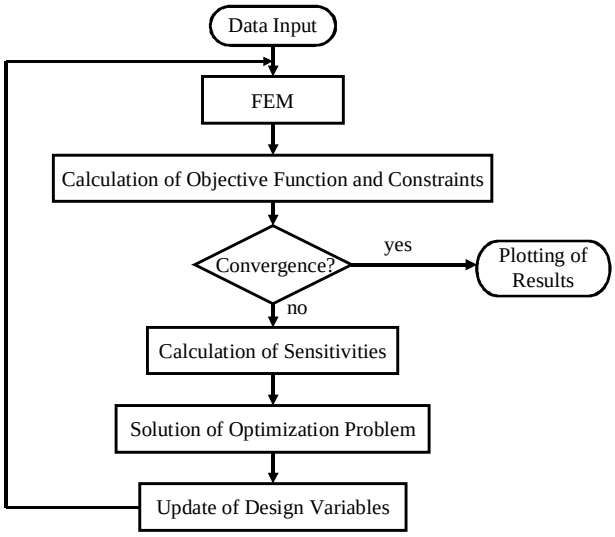

Figure 2 – Flowchart of the TOM algorithm.

The application of TOM is not recent and it began in the mechanical structural area, where the method demonstrated its great potentiality in the design of mechanical parts with maximum stiffness and smaller weight. Thus, it had been used broadly in the design of optimized parts at the automotive and aeronautics industries in the United States, Japan and Europe (Bendsøe and Sigmund, 2003). In those designs one of the considered materials is the "air", so the TOM allows us to design structures with positioned holes in great way such that maximize the structural rigidity with the smallest volume material as possible. There are several other types of designs whose nature makes attractive the application of TOM. Thereby, for instance, the TOM was applied recently for design of compliant mechanisms (Nishiwaki et al., 1998; Lima and Silva, 2001), composites materials (Kikuchi et al., 1998) and piezoelectric actuators (Silva et al., 2000).

4. Formulation and Implementation of the TOM applied to EIT

The image reconstruction by EIT using TOM can be interpreted as the problem of finding the material distribution inside the domain that reproduces the measured voltage values at electrodes, which are located on the boundary of the domain, when some cases of current are applied. The material distribution is directly related to the conductivity distribution in the domain. In that way, the optimization problem whose solution has been studied with TOM, could be:

$$\text{Minimize:} \quad F = \frac{1}{2}\sum_{j=1}^{ne}\sum_{i=1}^{np}\left(\phi_{ij} - \phi_{ij0}\right)^2 \tag{2}$$

such that: *electrical conductivity equation*

$$0 \le \rho_i \le 1 \quad i = 1...N$$

where F is the objective function related with the difference (to be minimized) between the values of electric potential measured on the electrodes (ϕ_{ij0}) and calculated in the computational model of the domain using finite elements (ϕ_{ij}). The *ne* and *np* values are the number cases of applied current load and the number of measurement points (electrodes), respectively, and ρ_i are the design variables related to the amount of material in each element of the domain.

The optimization problem above, Eq. (2), is an ill-posed problem whose its solution yields some local minimum, in other words, there are different distributions of conductivities in the domain that yield the same voltage values in the electrodes with same pattern of current excitement (Sylvester and Uhlmann, 1987). However, the application of TOM to that problem makes possible the inclusion of several constraints in the reconstruction image problem, restricting the solution space easily to that desired at clinic and avoiding images without clinical meaning.

4.1. FEM for conductive medium

In this work, the design domain is related to a body section whose image is desired. This domain is discretized by finite elements (see Fig. 3) where the electric potentials in all nodes are achieved by using FEM analysis with application of electric currents to the boundary nodes of the domain.

The FEM formulation applied to conductive medium (Muray and Kagawa, 1985) is generated from electrical conductivity equations, which are given by:

$$div\left(\sigma\nabla\phi\right) = 0 \text{ and } \begin{cases} \mathbf{I} = \sigma\nabla\phi \quad [\text{A/m}^2] \\ I_n = \sigma\nabla\phi.\mathbf{n} = \sigma\dfrac{\partial\phi}{\partial n} \quad [\text{A/m}^2] \end{cases} \tag{3}$$

where ϕ is the electric potential, σ is the electric conductivity, **n** is a normal vector to the boundary of domain, **I** is the electrical current vector (in ampere per square meter), I_n is a component of the electrical current in the direction **n**, *div* is the divergent operator and ∇ is the gradient operator.

Then, the FEM formulation consists in substituting approach functions of the electric potential into the integral form of the electric conductivity equations of Eq. (3). Thus, it is possible to calculate the electric potentials distributed in the discretized domain through a system of equilibrium equations, whose matrix formulation is given by:

$$\mathbf{K}\,\mathbf{\Phi} = \mathbf{I} \tag{4}$$

where $\mathbf{K}$ is the global FEM electric conductivity matrix of discretized domain, $\mathbf{\Phi}$ is a vector of nodal electric potential and $\mathbf{I}$ is a vector of nodal electric current. Equation (4) is a linear equation system that can be solved by using methods such as Gauss-Jordan, Conjugated Gradients and other (Bathe, 1996).

In fact, the nodal electric potential is obtained from electric current applied to nodes of electrode elements positioned in the boudary domain (see Fig. 3). In this way, the resistivity contact between the metal electrodes and patient skin, in clinical application with EIT, is simulated. In this work, an electrode model proposed by Hua et al. (1993) has been used. In addition to represent the distribution of the electric field for the contact interface, that model considers the dominant effects of the contact resistance of the electrodes.

The FEM model of the discretized domain uses quadrilateral elements whose electrical conductivity matrix ($\mathbf{k}_e$) is shown in Fig. 3, where **B** is the derivative of approach functions in relation to the cartesian coordinates and *h* is the thickness of the element. Electrode elements are also considered (see Fig. 3), in which the electric potential everywhere on a metal electrode (nodes 4, 5 and 6) is assumed to be equal ($\phi_4 = \phi_5 = \phi_6$). Then, the electrical conductivity matrix ($\mathbf{k}_{el}$) of the electrode element is shown in Fig. 3, where a is the half width of an electrode, t is the thickness of the contact interface (electrode-skin) and ρ is the resistivity (inverse of the conductivity) value of the contact interface. The insert of the electrode elements in the global matrix of the FEM analysis is made as the insert of the quadrilateral elements matrix.

4.2. Solution of the topology optimization problem

In this work, the optimization algorithm used to solve the problem of Eq. (2) is known as Sequential Linear Programming (SLP), which has been successfully applied to topology optimization. Among the advantages of SLP we can mention that it allows us to work with a large number of design variables and complex objective functions. Moreover, the SLP is easy to implement in computational algorithm. The SLP solves a non-linear optimization problem considering it as a sequence of linear sub-problems, which can be solved with Linear Programming (LP) (Haftka et al.,

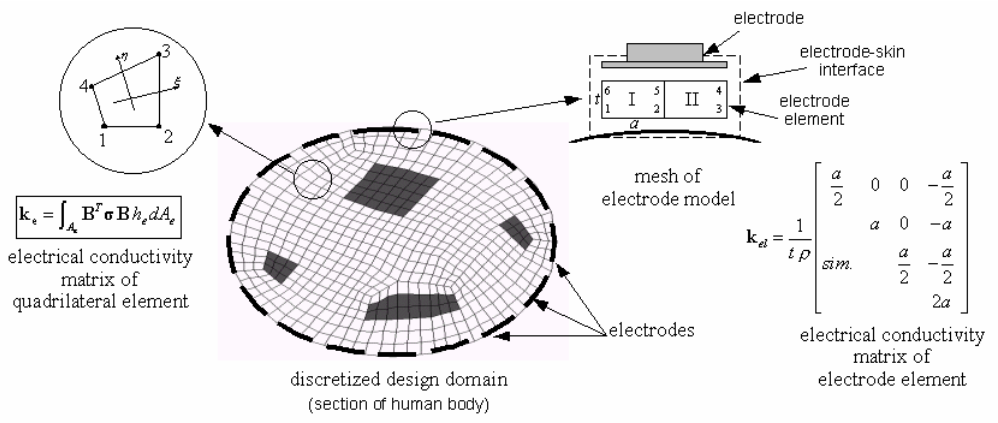

Figure 3 – Discretized domain and electrode model.

1996). The LP solves optimization problems whose objective function and constraints are linear functions of design variables.

The optimization problem of Eq. (2) can be linearized by writing a Taylor series expansion for the objective function and despising the terms with derivative of second or superior order. Thereby, the linear function to be minimized in LP is given by:

$$F^{\text{linear}} = \frac{\partial F}{\partial \rho_1}\bigg|_{\boldsymbol{\rho}=\boldsymbol{\rho}^0} \rho_1 + \frac{\partial F}{\partial \rho_2}\bigg|_{\boldsymbol{\rho}=\boldsymbol{\rho}^0} \rho_2 + \ldots + \frac{\partial F}{\partial \rho_n}\bigg|_{\boldsymbol{\rho}=\boldsymbol{\rho}^0} \rho_n \tag{5}$$

The coefficients of the variables ρ_i shown in Eq. (5) are the gradients (or derivates) of the objective function relative to design variables of the problem, in the point $\boldsymbol{\rho} = \boldsymbol{\rho}^0$. The calculation of these gradients is shown in the next section of this paper.

For that approach to be valid it is necessary to limit the variation of value of the design variables in each linear sub-problem by using of moving limits (Haftka et al., 1996). Typically, during one iteration, the design variables will be allowed to change by around 15% of their original values. Therefore, in each iteration, the SLP algorithm minimizes the linear sub-problem in the interval of the moving limits and it finds the optimum value for the variable, that it will be used in the following iteration. Thereby, iterations proceed successively, using the optimum value of the design variables having found in the iteration as initial value of the subsequent iteration, up to convergence of the solution.

4.3. Sensitivity analysis

The gradients (or derivatives) of the objective function and constraints are known as sensitivities of topology optimization problem. These gradients are used in the SLP for obtaining the linear sub-problems. In this work, the mathematical formulation of the gradients of Eq. (5) is obtained using the mutual energy concept (Byun et al., 1999).

Applying the chain rule to the Eq. (2), the derivative of the objective function in relation to design variables (ρ) of the optimization problem, can be written in the following form:

$$\frac{dF}{d\rho} = \frac{\partial F}{\partial \phi_{ij}} \frac{\partial \phi_{ij}}{\partial \rho} = \sum_{j=1}^{ne} \sum_{i=1}^{np} \left(\phi_{ij} - \phi_{ij0}\right) \frac{\partial \phi_{ij}}{\partial \rho} \tag{6}$$

The derivative of the Eq. (6) is determined by using the Maxwell's reciprocity theorem (Cook e Young, 1985) where if it is assumed that a body is submitted simultaneously to two cases of applied current load, the mutual energy concept is verified. Then we can express it in a matrix form, using problem discretized by FEM formulation, in the following way:

$$\mathbf{I}_1^T \boldsymbol{\Phi}_2 = \mathbf{I}_2^T \boldsymbol{\Phi}_1 \tag{7}$$

where $\mathbf{I}$ is the applied current electric vector, $\boldsymbol{\Phi}$ is the potential electric vector, the index $_1$, $_2$ indicates first and second case of applied current load and ^{T} indicates the transposition of the vector. Initially, we admit a fictitious excitement $\mathbf{I}_2$ as a current electric vector whose only non-zero component is a unit current applied to one point of the body, that is:

$$\mathbf{I}_2^T = \{0 \quad 0 \quad 0 \quad \cdots \quad 1 \quad \cdots \quad 0 \quad 0\} \tag{8}$$

Using equilibrium equation from FEM formulation ($\mathbf{K}\,\mathbf{\Phi} = \mathbf{I}$) which relates current and electric potential vectors (Bathe, 1996), and using the Eq. (8), we obtain:

$$\mathbf{\Phi}_1^{\mathrm{T}}\,\mathbf{K}\,\mathbf{\Phi}_2 = \phi_1 \qquad (\textit{mutual energy of the system}) \tag{9}$$

where $\mathbf{K}$ is the symmetrical global matrix which $\mathbf{K}^{\mathrm{T}} = \mathbf{K}$ and $(\mathbf{K}^{-1})^{\mathrm{T}} = \mathbf{K}^{-1}$. From derivation of two sides of the Eq. (9) relative to design variables of the problem optimization, we obtain:

$$\frac{\partial\left(\mathbf{\Phi}_1^{\mathrm{T}}\,\mathbf{K}\,\mathbf{\Phi}_2\right)}{\partial\rho} = \frac{\partial\left(\phi_1\right)}{\partial\rho} \tag{10}$$

The gradient of the left side of the Eq. (10) is the derivative of the mutual energy of the system, which is developed of the following form:

$$\frac{\partial\left(\mathbf{\Phi}_1^{\mathrm{T}}\,\mathbf{K}\,\mathbf{\Phi}_2\right)}{\partial\rho} = \frac{\partial\mathbf{\Phi}_1^{\mathrm{T}}}{\partial\rho}\mathbf{K}\,\mathbf{\Phi}_2 + \mathbf{\Phi}_1^{\mathrm{T}}\frac{\partial\mathbf{K}}{\partial\rho}\mathbf{\Phi}_2 + \mathbf{\Phi}_1^{\mathrm{T}}\,\mathbf{K}\frac{\partial\mathbf{\Phi}_2}{\partial\rho} \tag{11}$$

Deriving the equilibrium equation $\mathbf{K}\,\mathbf{\Phi}_1 = \mathbf{I}_1$ (first load case) relative to design variables, we have:

$$\frac{\partial\mathbf{K}}{\partial\rho}\mathbf{\Phi}_1 + \mathbf{K}\frac{\partial\mathbf{\Phi}_1}{\partial\rho} = \frac{\partial\mathbf{I}_1}{\partial\rho} \tag{12}$$

However, the electric current vector $\mathbf{I}_1$ does not change with design variables, then:

$$\frac{\partial\mathbf{K}}{\partial\rho}\mathbf{\Phi}_1 + \mathbf{K}\frac{\partial\mathbf{\Phi}_1}{\partial\rho} = 0 \quad \Rightarrow \quad \frac{\partial\mathbf{\Phi}_1}{\partial\rho} = -\mathbf{K}^{-1}\frac{\partial\mathbf{K}}{\partial\rho}\mathbf{\Phi}_1 \tag{13}$$

Thus, transposing the Eq. (13), we obtain:

$$\frac{\partial\mathbf{\Phi}_1^{\mathrm{T}}}{\partial\rho} = -\mathbf{\Phi}_1^{\mathrm{T}}\frac{\partial\mathbf{K}^{\mathrm{T}}}{\partial\rho}\left(\mathbf{K}^{-1}\right)^{\mathrm{T}} \quad \Rightarrow \quad \frac{\partial\mathbf{\Phi}_1^{\mathrm{T}}}{\partial\rho} = -\mathbf{\Phi}_1^{\mathrm{T}}\frac{\partial\mathbf{K}}{\partial\rho}\mathbf{K}^{-1} \tag{14}$$

Likewise, deriving the equilibrium equation $\mathbf{K}\,\mathbf{\Phi}_2 = \mathbf{I}_2$ (second load case), we obtain:

$$\frac{\partial\mathbf{\Phi}_2}{\partial\rho} = -\mathbf{K}^{-1}\frac{\partial\mathbf{K}}{\partial\rho}\mathbf{\Phi}_2 \tag{15}$$

Substituting equations (14) and (15) in the Eq. (11) and simplifying:

$$\frac{\partial\left(\mathbf{\Phi}_1^{\mathrm{T}}\,\mathbf{K}\,\mathbf{\Phi}_2\right)}{\partial\rho} = -\,\mathbf{\Phi}_1^{\mathrm{T}}\frac{\partial\mathbf{K}}{\partial\rho}\mathbf{\Phi}_2 \qquad (\textit{gradient of the mutual energy}) \tag{16}$$

Thus, the Eq. (10) can be written in the following way:

$$-\,\mathbf{\Phi}_1^{\mathrm{T}}\frac{\partial\mathbf{K}}{\partial\rho}\mathbf{\Phi}_2 = \frac{\partial\phi_1}{\partial\rho} \tag{17}$$

In the EIT, some measurements (i = 1 to *np*) around of the body section in different points (electrodes) are made for one case of applied current load. Thus, we consider the configuration for the first measurement point (i = 1) shown in Fig. 4. Now, the fictitious excitement of the Eq. (8) is considered a vector whose components are:

$$\mathbf{I}_{1\mathrm{j}}^{\mathrm{T}} = \left\{(\phi_{1\mathrm{j}} - \phi_{1\mathrm{j}0}) \quad 0 \quad 0 \quad \cdots \quad 0\right\} \tag{18}$$

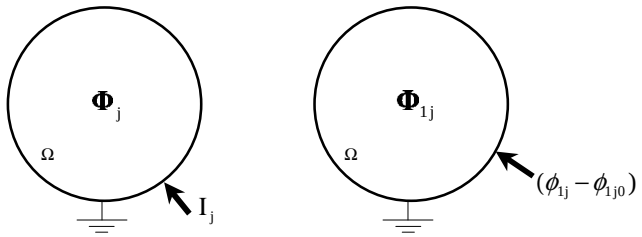

Figure 4 – Application to the first measurement point.

This current electric vector, Eq. (18), produces in the domain Ω a potential field $\boldsymbol{\Phi}_{1\mathrm{j}}$. It is known that the current electric $(\phi_{1\mathrm{j}} - \phi_{1\mathrm{j}0})$ is constant during the load case. Thus, applying the equation (17) we have:

$$-\boldsymbol{\Phi}_{\mathrm{j}}^{\mathrm{T}} \frac{\partial \mathbf{K}}{\partial \rho} \boldsymbol{\Phi}_{1\mathrm{j}} = (\phi_{1\mathrm{j}} - \phi_{1\mathrm{j}0}) \frac{\partial \phi_{1\mathrm{j}}}{\partial \rho} \tag{19}$$

Then, if the procedure is repeated in analogous way to the first measurement until completing *np* measurement points, we have:

$$-\boldsymbol{\Phi}_{\mathrm{j}}^{\mathrm{T}} \frac{\partial \mathbf{K}}{\partial \rho} \boldsymbol{\Phi}_{npj} = (\phi_{npj} - \phi_{npj0}) \frac{\partial \phi_{npj}}{\partial \rho} \tag{20}$$

Now, we consider the development of the first summation (1 to *np*) of the Eq. (6):

$$\frac{\mathrm{dF}}{\mathrm{d}\rho} = \sum_{\mathrm{j}=1}^{ne} \left[\left(\phi_{1\mathrm{j}} - \phi_{1\mathrm{j}0}\right) \frac{\partial \phi_{1\mathrm{j}}}{\partial \rho} + \left(\phi_{2\mathrm{j}} - \phi_{2\mathrm{j}0}\right) \frac{\partial \phi_{2\mathrm{j}}}{\partial \rho} + \cdots + \left(\phi_{npj} - \phi_{npj0}\right) \frac{\partial \phi_{npj}}{\partial \rho} \right] \tag{21}$$

By comparison of the Eq. (21) with the development for obtain Eq. (20) and considering *np* measurement points, we conclude:

$$\frac{\partial \mathrm{F}}{\partial \rho} = -\sum_{\mathrm{j}=1}^{ne} \left(\boldsymbol{\Phi}_{\mathrm{j}}^{\mathrm{T}} \frac{\partial \mathbf{K}}{\partial \rho} \boldsymbol{\Phi}_{1\mathrm{j}} + \boldsymbol{\Phi}_{\mathrm{j}}^{\mathrm{T}} \frac{\partial \mathbf{K}}{\partial \rho} \boldsymbol{\Phi}_{2\mathrm{j}} + \cdots + \boldsymbol{\Phi}_{\mathrm{j}}^{\mathrm{T}} \frac{\partial \mathbf{K}}{\partial \rho} \boldsymbol{\Phi}_{npj} \right) \tag{22}$$

Grouping the similar terms of the Eq. (22), we have:

$$\frac{\partial \mathrm{F}}{\partial \rho} = -\sum_{\mathrm{j}=1}^{ne} \boldsymbol{\Phi}_{\mathrm{j}}^{\mathrm{T}} \frac{\partial \mathbf{K}}{\partial \rho} \underbrace{\left(\boldsymbol{\Phi}_{1\mathrm{j}} + \boldsymbol{\Phi}_{2\mathrm{j}} + \cdots + \boldsymbol{\Phi}_{npj} \right)}_{\boldsymbol{\Phi}_{2\mathrm{j}}^{"}} \tag{23}$$

As the FEM formulation in this case is linear, we can get the summation of potentials $\boldsymbol{\Phi}_{2\mathrm{j}}^{"}$ applying all *np* measurement points, simultaneously, using a vector current electric like that:

$$(\mathbf{I}_{2\mathrm{j}}^{"})^{\mathrm{T}} = \mathbf{I}_{1\mathrm{j}}^{\mathrm{T}} + \mathbf{I}_{2\mathrm{j}}^{\mathrm{T}} + \mathbf{I}_{3\mathrm{j}}^{\mathrm{T}} + \cdots + \mathbf{I}_{npj}^{\mathrm{T}} = \left\{ (\phi_{1\mathrm{j}} - \phi_{1\mathrm{j}0}) \quad (\phi_{2\mathrm{j}} - \phi_{2\mathrm{j}0}) \quad (\phi_{3\mathrm{j}} - \phi_{3\mathrm{j}0}) \quad \cdots \quad \cdots \quad (\phi_{npj} - \phi_{npj0}) \right\} \tag{24}$$

Thus, the vector $\boldsymbol{\Phi}_{2\mathrm{j}}^{"}$ can be calculated through the equilibrium equation $\mathbf{K}\, \boldsymbol{\Phi}_{2\mathrm{j}}^{"} = \mathbf{I}_{2\mathrm{j}}^{"}$.

Therefore, considering *ne* applied load cases and *np* measurement points, the expression to calculate of derivative of the objective function is given by:

$$\frac{\mathrm{dF}}{\mathrm{d}\rho} = \sum_{\mathrm{j}=1}^{ne} \sum_{\mathrm{i}=1}^{np} \left(-\boldsymbol{\phi}_{\mathrm{j}}^{\mathrm{T}} \frac{\partial \mathbf{K}}{\partial \rho} \boldsymbol{\phi}_{\mathrm{ij}}^{*} \right) \tag{25}$$

Thus, this procedure saves a lot of computational time to calculate the gradients of the objective function relative to design variables.

5. Results

The topology optimization problem for obtaining image by EIT is implemented in a software programmed using C language. In this section, some examples will be presented to illustrate image reconstruction through that software. Figure 5a shows the image that will be reconstructed here (numerical phantom). In this case, the dark and clear region simulates a material with low conductivity (10^{-5} $(\Omega m)^{-1}$) and high conductivity (5.10^{-3} $(\Omega m)^{-1}$), respectively. In practice, this situation would be equivalent for obtaining one region with presence of air in the tomography of an water like domain, for instance.

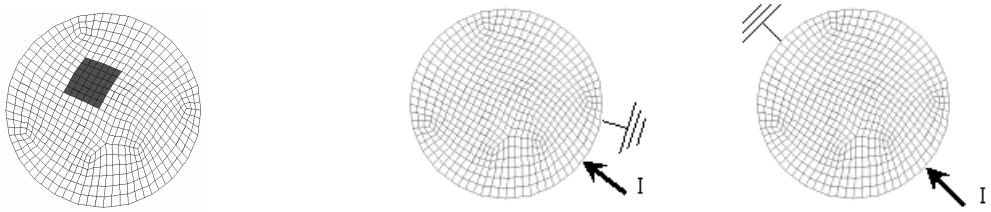

a) imagem desired b) adjacent pattern c) diametral pattern

Figure 5 – Image to be reconstructed and electric excitement patterns in EIT.

The image is obtained from circular domain whose diameter measurement is 500 millimeters. That domain is discretized by 567 quadrilateral finite elements (thickness = 35 millimeters) using mesh generator of ANSYS software. In this work, for obtaining a good quality image to clinical application of the EIT, 32 electrode elements are used on outline of the design domain, according to Cheney et al. (1999). To find the nodal electric potentials in those electrode elements a pair of them is excited electrically, following a certain pattern which can be adjacent or diametral (see Fig. 5b e 5c), where one of them is made to be null potential ("ground") and the other receives the low frequency electric current.

Thereby for obtaining the image desired in the EIT, the pair of electrodes is changed successively until getting enough number of observations under different angles. Therefore, in total, a sequence of 32 patterns of electric excitement of same type (adjacent or diametral) is applied to image reconstruction here. For all examples shown in this section, the applied electric current is considered equal to 1 milliampere, the width of electrode elements is 9 millimeters. Moreover, in these examples, the topology optimization was performed considering the penalization parameter p is equal to 2 and using 0.15 as initial value for design variables at starting of the SLP. In this work, the measured electric potential, which will be used for calculating the objective function, were obtained through numerical phantom. To follow, the images gotten by applying adjacent and diametral pattern are shown.

5.1. Images obtained from applying adjacent pattern

Figure 6 shows image and convergence curve gotten by applying the adjacent pattern of electric excitement. In the graph of Fig. 8a, the absolute conductivity values of elements in the dark region (material with low conductivity) are shown.

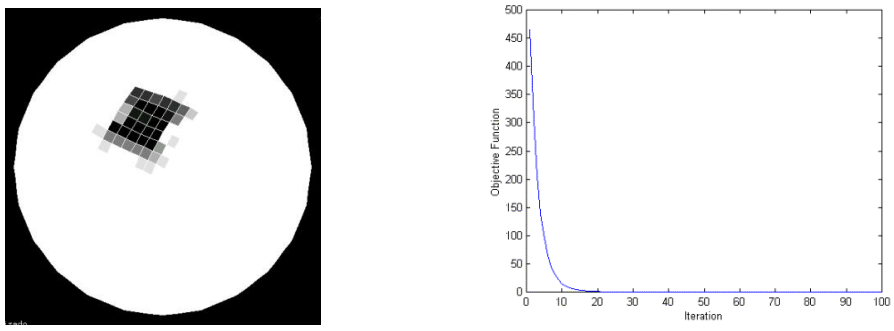

a) image tomography b) convergence curve

Figure 6 – Obtained image and convergence curve (adjacent pattern).

5.2. Images obtained from applying diametral pattern

For comparison, the obtained image and convergence curve from applying the diametral pattern of electric excitement are shown in Fig. 7.

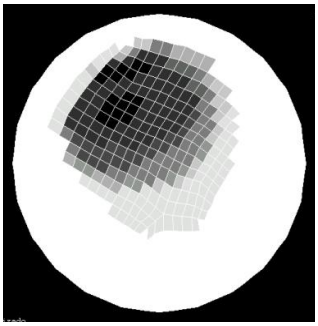

a) image tomography

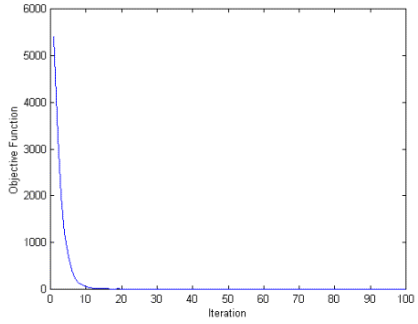

b) convergence curve

Figure 7 – Obtained image and convergence curve (diametral pattern).

The absolute conductivity values of elements in the dark region are shown in the graph of Fig. 8b.

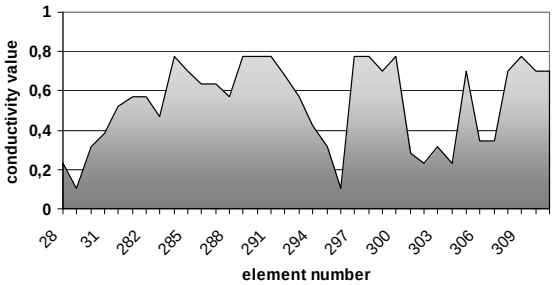

a) values to the dark region of Fig. 6a

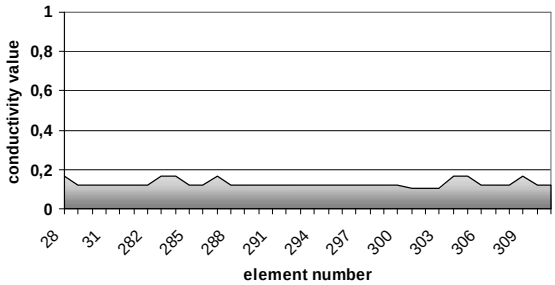

b) values to the dark region of the Fig. 7a

Figure 8 – Conductivity values ($x10^{-5}$) of dark region.

5.3. Discussion

According to results presented here, we can verify that the software is able to obtain the images of the example considered with a certain level of image resolution acceptable, where the absolute electric conductivity values of dark region were getting on average of 80% of the expected original value to adjacent pattern case and 20% (approximately) to diametral pattern case. Observing the comparison between the two patterns of electric excitement it is noticed that the adjacent pattern was more appropriate for the examples presented here, because images resolution generated is better than one generated by the diametral pattern. Other researchers using other methods had the same conclusion presented here (Cheney et al., 1999). According to convergence graphs it is verified that the objective functions in both cases (adjacent and diametral) fell in quick near at minimum value (10 iterations approximately), however they continue iteration by iteration with very small oscillation until the best image for the tomograpy examination is found. Although both cases have been made to run to the same iteration limit (100) it is also noticed for adjacent pattern case the objective function converges to a minimum value (~0,01) smaller than the diametral pattern minimum value (~1,65). The optimization of the diametral pattern case fell in an optimum local that we believe could be improved. Thus, still it is premature to affirm that the adjacent pattern case will be better for all cases. Therefore, more research and study will be conducted to inquire this fact.

6. Conclusions

An algorithm of topology optimization applied to EIT was proposed for obtaining tomography images. This implementation utilizes a FEM model with electrode elements that consider the electric contact resistance between the metal electrodes and the human body, an objective function commonly applied to solve the inverse problem of EIT, a method to calculate the sensitivity of the objective function based on concepts of mutual energy, a material model based on density method for the mixture of two materials, and an optimization algorithm based on SLP. The software written in C language was implemented to accomplish the iterative process of TOM. The images, shown in section 5, were obtained from voltage values obtained from numerical phantom. In this way, the results presented here demonstrate that the software is able to obtain in some sets of ten iterations the values of absolute conductivity of two materials inside of the domain. However it is still necessary to improve it to work with data obtained through experimental phantom (with noise).

The algorithm of TOM, studied in this work, could be seized for obtaining images of the lung through EIT device. The TOM allows us to include some restrictions in the problem of image reconstruction limiting the solution space and avoiding images without clinical meaning. For instance, it can be limited in the design domain the area which presence

of air in the lung can occur, besides allowing to work with known areas inside the domain (bone, heart, etc).

7. Acknowledgement

First author thanks the financial support of FAPESP through doctoral scholarship (n°. 02/01625-0).

8. References

Amato, M.B.P., 2001, “Novas Estratégias em Ventilação Artificial: Diagnóstico e Prevenção do Barotrauma/ Biotrauma Através da Tomografia de Impedância Elétrica”, Sumário do Projeto Temático FAPESP (n° 01/05303-4).

Barber, D.C., 1990, “Quantification in Impedance Imaging”. Institute of Physical Sciences in Medicine Clin. Phys. Physiol. Meas., vol.11, Suppl. A, 45-56.

Barber, D.C. and Brown, B.H., 1984, “Applied Potencial Tomography”. The Institute of Physics J. Phys. E: Sci. Instrum., vol.17, 723-733.

Bathe, K.J., 1996, "Finite Elements Procedures", Prentice Hall, New Jersey.

Bendsøe, M. P. and Kikuchi, N., 1988, “Generating Optimal Topologies in Structural Design Using a Homogenization Method”. Computer Methods in Applied Mechanics and Engineering, 71, 197-224.

Bendsøe, M. P. and Sigmund, O., 1999, “Material Interpolations Schemes in Topology Optimization”, Archive of Applied Mechanics, vol. 69, 635-654.

Bendsøe, M. P. and Sigmund, O., 2003, “Topology Optimization: Theory, Methods and Applications”, Springer-Verlag, New York.

Byun, J.K.; Lee, J.H.; Park, I.H.; Lee, H.B.; Choi, K. and Hahn S.Y., 1999, “Inverse Problem Application of Topology Optimization Method with Mutual Energy Concept and Design Sensitivity”, Proceed. of IEEE Magnetic, 296-300.

Cheney, M. and Isaacson, D., 1991, “An Overview of Inversion Algorithms for Impedance Imaging”, Inverse Scattering and Applications, O.H.Sattinger, C.A.Tracy, and S. Venakides, eds., AMS, Providence, RI.

Cheney, M.; Isaacson, D. and Newell, J.C., 1999, “Electrical Impedance Tomography”, SIAM review, 41, no.1, 85-101.

Cheney, M.; Isaacson, D.; Newell, J.C.; Goble J. and Simske S., 1990, “NOSER: An Algorithm for Solving the Inverse Conductivity Problem”, Internat. J. Imaging Systems and Technology, 2, 66-75.

Cook, R. D. and Young, W. C., 1985, “Advanced Mechanics of Materials”, Macmillan, New York.

Guardo, R.; Boulay, C.; Murray, B. and Bertrand, M., 1991, “An Experimental Study in Electrical Impedance Tomography Using Backprojection Reconstruction”. IEEE Transactions on Biomedical Eng., 38, n.7, 617-627.

Haftka, R.T.; Gürdal, Z. and Kamat, M.P., 1996, "Element of Structural Optimization", Kluwer Academic Publishers, Boston.

Holder, D., 1993, “Clinical and Physiological Applications of Electrical Impedance Tomography”, UCL, Press, London.

Hua, P.; Woo, E.J.; Webster, J.G. and Tompkins, W.J., 1993, “Finite Element Modeling of Electrode-Skin Contact Impedance in Electrical Impedance Tomography”, IEEE Transactions on Biomedical Engineering, 40, 335-343.

Isaacson, D.; Cheney, M. and Newell, J. C., 1992, “Comments on Reconstruction Algorithms”, Institute of Physical Sciences in Medicine Clin. Phys. Physiol. Meas., vol.13, Suppl. A, 83-89.

Kikuchi, N.; Nishiwaki, S.; Fonseca, J.S.O. and Silva, E.C.N., 1998, “Design Optimization Method for Compliant Mechanisms and Material Microstructures”, Computer Methods in Applied Mechanics and Eng., 4, 151, 401-417.

Lima, C.R. and Silva, E.C.N., 2001, “Projeto de Mecanismos Flexíveis Usando o Método de Otimização Topológica”, Anais do XVI Cobem’2001, Uberlândia, Brasil.

Muray, T. and Kagawa, Y., 1985, “Electrical Impedance Computed Tomography Based on a Finite Elements Model”, IEEE Trans. Biomed. Eng., 32.

Nishiwaki, S.; Frecker, M.I.; Min, S. and Kikuchi, N., 1998, “Topology Optimization of Compliant Mechanisms using the Homogenization Method”, International Journal of Numerical Methods in Engineering, 42, 535-559.

Paulson, K.; Breckon, W. and Pidcock, M. A., 1992, “Hybrid Phantom for Impedance tomography”. Institute of Physical Sciences in Medicine Clin. Phys. Physiol. Meas., vol. 13, Suppl. A, 155-159.

Santosa F. and Vogelius M., 1990, “A Backprojection Algorithm for Electrical Impedance Imaging”, SIAM J. Appl. Math., 50, 216-243.

Silva, E.C.N.; Nishiwaki, S. and Kikuchi, N., 2000, “Topology Optimization Design of Flextensional Actuators”, IEEE Transactions on Ultrasonics, Ferroelectrics and Frequency Control, 47, 3, 657-671.

Simske, S., 1987, “An Adaptive Current Determination and a One-Step Reconstruction Technique for Current Tomography System”, Master´s Thesis, Rensselaer Polytechnic Institute, Troy, NY.

Sylvester, J. and Uhlmann, G. A., 1987, “Global Uniqueness Theorem for an Inverse Boundary Value Problem”, Annals of Mathematics, 125, 153-169.